Technical Document 3227
May 2008

Ray-Optics-Based Signal Strength Prediction Method for the Earth-to-Satellite Propagation Model with Meteorology (ESPM2) in the Advanced Refractive Effects Prediction System

R. Sprague

SSC Pacific
San Diego, CA 92152-5001

Technical Document 3227
December 2011

Ray-Optics-Based Signal Strength Prediction Method for the Earth-to-Satellite Propagation Model with Meteorology (ESPM2) in the Advanced Refractive Effects Prediction System

R. Sprague

SSC Pacific
San Diego, CA 92152-5001

SSC Pacific
San Diego, California 92152-5001

J.J. Beel, CAPT, USN
Commanding Officer

C. A. Keeney
Executive Director

ADMINISTRATIVE INFORMATION

This report was prepared for the office of Naval Research (ONR) by the Atmospheric Propagation Branch (Code 55480) of the Electromagnetics & Advanced Technology Division (Code 237), SSC Pacific.

Released by
D. Tsintikidis, Head
Atmospheric Propagation Branch

Under authority of
S. Russell, Head
Electromagnetics & Advanced
Technology Division

SB

CONTENTS

I. INTRODUCTION

The Advanced Refractive Effects Prediction System (AREPS) was initially developed as a performance assessment and system analysis tool for U.S. Navy radar systems operating in the 100 MHz to 20 GHz frequency range. Recently, under major funding from the Office of Naval Research (ONR), AREPS capabilities have been extended to include high frequency (HF, 2-30 MHz) point-to-point and coverage predictions in support of military communication systems and a fully three-dimensional ionospheric ray tracing capability for research oriented and system design applications at HF. Continuing this effort at expanding the frequency and application range of AREPS, we have recently developed a medium prediction capability for coverage analysis in the AM (300 kHz- 2 MHz) radio band.

With these additions we have extended the AREPS usable prediction frequency range from 300 kHz to 57 GHz and have added significant communication system analysis capability. In this document, we will describe the latest efforts to extend the range of applications of AREPS to earth-satellite communications. The new capability, to be called the Earth-to-Satellite Propagation with Meteorology Model ($ESPM^2$), employs a ray optics propagation model, including available meteorological/refractivity data, to predict signal strength at satellite locations. Propagation based loss mechanisms considered in the signal strength determination include gaseous absorption and absorption due to rain on the propagation path. Since we intend the module to be usable for both geo-stationary and orbiting satellites, we have also included an orbital prediction capability which allows locations and time-of-availability to be determined for almost any satellite.

This document is intended as a description of the ray optics methods which have been developed for use in signal strength prediction in $ESPM^2$. We also include a short discussion (including references to more detailed descriptions) of the pre-existing models chosen for prediction of losses due to gaseous and rain absorption, as they directly affect the signal strength calculation. For completeness, we also provide a short discussion of the orbital prediction model (with references) and illustrate its usefulness in $ESPM^2$. In the following section we discuss, generally, the refractive model that is used in the ray optics program. Details of how and where these refractive profiles are obtained within AREPS are described elsewhere.

II. ATMOSPHERIC REFRACTIVITY AND MODEL INPUT

An electromagnetic wave propagating in the earth's atmosphere feels the effects of bound electrons in the molecular species which make up the atmosphere. Under the action of the electric field of the passing wave, a time varying induced field is created which radiates a secondary field that, when combined with the original wave, may cause the path of the original wave to change. This change in the original path is called refraction and, under certain conditions, may cause large deviations of the intended direction of the original wave. For the wave frequencies used in satellite communications and the nominal molecular density of the lower atmosphere, it is usually the case that the

effects of refraction can be ignored and the effect of the atmosphere on system performance is restricted to losses due to rain and, to a lesser extent, gaseous absorption of wave energy. However, the refractive effects of the atmosphere can become anomalously large under certain atmospheric conditions of temperature, pressure and humidity (ducting) and the refractive effects then dominate all other propagation effects, essentially determining if communication is possible at all. Also, when a satellite appears low on the horizon, the path of the wave through the atmosphere is very long and the cumulative refractive effects can be large even under normal refractive conditions. It is for these anomalous conditions that the ESPM^2 module is expected to be most useful.

For the purposes of this document, we assume the refractive structure of the atmosphere on the propagation path between transmitting antenna and receiving antenna (assumed throughout this document to be at the satellite) is known. In general, the atmosphere varies in both height and range and the ray optics model described here allows for both. To include the range dependence in a consistent way, we make the following definitions regarding the propagation path.

Consider the plane containing the transmitter antenna site, the instantaneous receiver site and the earth's center. We define the propagation region as the interior portion of the plane bounded by radials from the earth's center through the transmitter and receiver sites. Within this region, we further define sectors as sub-regions of the propagation region within which the earth's refractivity can be considered to be dependent on height only. Formally, let r_k be that radial within a sector 'k' such that the refractivity changes most 'quickly' as we move from the sector boundary along the θ-coordinate within the sector, keeping r_k fixed. For this fastest changing radial, we define the angle ψ_k to be the angle subtended at the earth's center over which the refractivity is approximately constant. The angle ψ_k defines the angular range of the kth-sector. Repeating this process throughout the propagation region for sequential sectors, the angular range of the region, ψ_s, which is also the angle subtended between the transmit antenna and the satellite, can be written

$$\psi_s = \sum_{k=1}^{K} \psi_k \qquad (1)$$

where K is the total number of sectors that make up the region. For each sector the refractivity is assumed to be dependent on height only. We note that this formal process for defining the sectors is impractical in practice, and the sectors are generally defined based on the availability of data or the user's tolerance for model execution time.

The input to the ray trace program then, consists of a height profile of refractivity $(N(i),Z(i))$, i= 1,..,L, where $Z(1)=0$, $Z(\mathrm{L})=H_s$ is the height in kilometers of the satellite above mean sea level and L is the number of refractivity samples, for each of the sectors which make up the propagation region. For heights above 50 km we assume the earth's atmosphere can be well approximated as vacuum and take $N(i)=0$ for $Z(i) > 50$ km. For heights below 50 km we further assume that $Z(i)$ can be adequately approximated by $r(i)$, where r is the radial coordinate in a spherical coordinate system referenced to the earth's

center. So at all heights we assume we can make the approximation that $N(Z(i)) \sim N(r(i))$ where $r(i)=r_e+Z(i)$ and r_e is the earth's radius (K.D. Anderson, 2000; A.R. Lowry, et al., 2002).

We also require specification of the transmitter height, T, in kilometers and the angle ψ_s between the sub-transmitter and sub-satellite points, subtended at the earth's center. The angle ψ_s, which can be alternately specified as ground range between the sub-terminal points, defines the propagation region. The height of the satellite H_s is also assumed to be known at all times and may be determined by the satellite orbit prediction software or input, if known to acceptable accuracy by the user, i.e. geo-stationary satellite.

The calculation of signal strength requires estimation of propagation losses. The model included for estimation of the gaseous absorption requires input of the height profile of the absorption rate. In practice, this profile is included at each height along with the refractivity. The rain attenuation loss is dependent on the geographical location of the transmit antenna and so we also require the latitude and longitude coordinates as input.

III. RAY CALCULATIONS

1. Basic Ray Equation for Range Independent Refractivity

In the description of the ray tracing program within this section we will assume that the transmitter is always located at a lower height than the receiver, which is assumed to be the satellite. Given the symmetry of the ray tracing method we could interchange terminology and the determined rays would remain unchanged. However, for purposes of this discussion we will use 'transmitter' to refer to the lower terminal and 'receiver' to refer to the satellite.

The geometry of the ray trace problem for a propagation region consisting of a single refractive sector (or for a single sector in a multiple sector region) is shown in Figure 1. Since the refractivity is a function of height z (or radial length r) only within a sector, the ray will remain in the initial azimuthal plane, which we take to be the φ =0 plane. In Fig.. 1, an initially up-going ray is launched at local zenith angle θ_0 (< 90°) from a transmitting antenna located at the point (r_T,0,0) in a spherical coordinate system referenced to the earth's center. Here $r_T=r_e$+T and r_e is the mean earth's radius. The problem then is to find the path of this ray through the specified height-dependent refractivity structure.

In Fig. 1 we focus on the ray as it passes through a spherical atmospheric layer bounded by $r=r(i)\equiv r_i$ and $r=r(i+1)\equiv r_{i+1}$. We assume the ray enters the layer at local zenith angle θ_i and passes through the layer. Then, if ds is an infinitesimal section of the ray at radial distance r ($r_i \le r < r_{i+1}$) making a zenith angle θ to the local radial (see figure 1), we can write (J.M. Kelso, 1964)

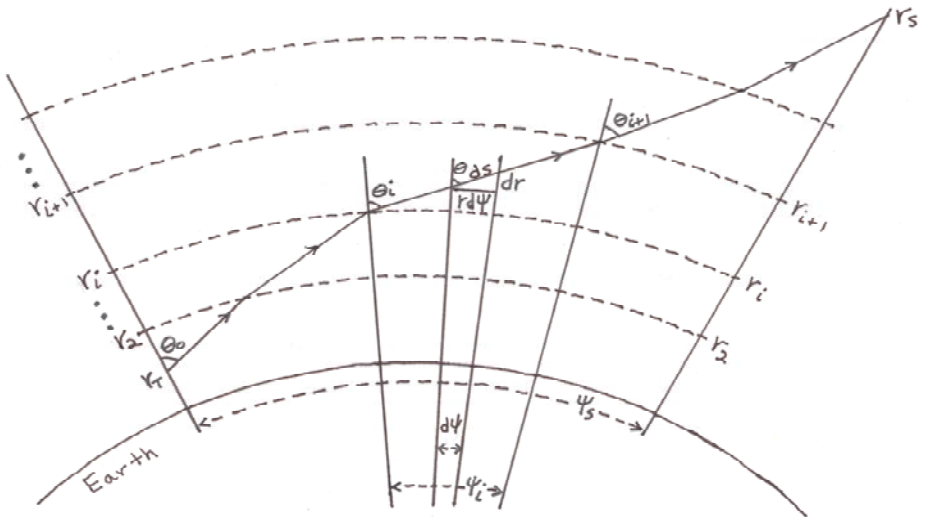

Figure 1. Ray launched at angle θ_0 which passes through the layer at r_i . The angle ψ_s is the angle subtended between the transmitter at (r_T,0,0) and the satellite located at (r_S,ψ_S,0).

$$r\frac{d\psi}{dr} = \tan\theta = \frac{\sin\theta}{\sqrt{1-\sin^2\theta}}\ , \tag{2}$$

where $d\psi$ is the angle subtended at the center of the earth by ds.

We next apply Bouger's Law (Snell's Law equivalent for spherical geometry), which states that

$$n(r)r\sin\theta = n(r_i)r_i\sin\theta_i = n_0 r_T\sin\theta_0\,, \tag{3}$$

in (2) to obtain

$$r\frac{d\psi}{dr} = \frac{n_i r_i\sin\theta_i}{\sqrt{n(r)^2r^2 - n_i^2 r_i^2\sin^2\theta_i}}\,. \tag{4}$$

Here $n(r)$ is the index-of-refraction at the radial distance r which is obtained from the refractivity $N(r)$ by the relation

$$N(r) = (n(r)-1)10^6\,, \tag{5}$$

and $n_i \equiv n(r_i)$ is the index at the bottom of the layer. We then obtain the total angle subtended by the ray in passing through the layer by integrating (4)

$$\psi\,|_{r_i}^{r_{i+1}} = \frac{n_i \sin\theta_i}{r_i} \int_{r_i}^{r_{i+1}} (\frac{r_i}{r})^2 \frac{dr}{\sqrt{n^2(r) - (\frac{r_i}{r})^2 n_i^2 \sin^2\theta_i}}, \quad r_i \le r < r_{i+1} \qquad (6)$$

Equation (6) is the basic ray equation evaluated in the ray trace model.

2. Evaluation of the Basic Ray Equation

One of our goals in solving the basic ray equation (6) is minimization of the computation time required to obtain a solution. This is especially important in light of the homing procedure to be discussed below which generally requires many evaluations of the basic ray equation to obtain a solution for a small error tolerance. Minimization of computation time can be partially accomplished by making simplifying assumptions in the integrand in order to cast (6) into a form for which closed form evaluation is possible.

The first simplification of (6) involves an approximation for the term $(r_i/r)^2$ which appears twice in the equation. We write this term as,

$$(\frac{r_i}{r})^2 = (\frac{r_e + z_i}{r_e + z})^2 = (\frac{r_e + z_i}{r_e + z_i + z - z_i})^2 = \frac{1}{(1+h)^2},$$

where $h=(z-z_i)/r_i$ and $z_i \le z < z_{i+1}$. We assume that h is much smaller than unity at all atmospheric heights and expand this term to obtain the approximation

$$(\frac{r_i}{r})^2 \approx 1 - 2h + 3h^2 - \ldots . \qquad (7)$$

We further simplify the ray equation by assuming that the refractivity is a linear function of height in the region between the layer boundaries and write $N(r)=N_i + S_i(r-r_i)$, where $r_i \le r < r_{i+1}$ and S_i is the constant refractivity slope in the i-th layer given by $S_i=(N_{i+1}-N_i)/(r_{i+1}-r_i)$. From (5) we can write the index-of-refraction in the layer as

$$\begin{aligned} n(r) &= n_i + s_i(r - r_i) \\ n_i &= 10^{-6} N_i + 1, s_i = 10^{-6} S_i \end{aligned} \qquad (8)$$

so, since (6) actually requires the square of the index-of-refraction, we have $n^2(h)= n_i^2 + 2s_i n_i r_i h + s_i^2 r_i^2 h^2$ where and $n_i^2=2n_i-1$.

With these simplifications the basic ray equation (6) can be written as

$$\psi\,|_{r_i}^{r_{i+1}} = C_0\left[\Gamma_1 - \frac{2}{r_i}\Gamma_2 + \frac{3}{r_i^2}\Gamma_3\right]$$

where $C_0=n_i\sin\theta_i$ and we have the following definitions,

$$\Gamma_1 = \int_0^{h_m} \frac{dh}{\sqrt{a+bh+ch^2}}, \Gamma_2 = \int_0^{h_m} \frac{hdh}{\sqrt{a+bh+ch^2}}, \Gamma_3 = \int_0^{h_m} \frac{h^2dh}{\sqrt{a+bh+ch^2}}, \qquad (9)$$

where $h_m=(z_{i+1}-z_i)/r_i$, $a=n_i^2\cos^2\theta_i$, $b=2n_is_ir_i + 2n_i^2\sin^2\theta_i$ and $c=s_i^2r_i^2 - 3n_i^2\sin^2\theta_i$. The integrals Γ_2 and Γ_3 can be written in terms of Γ_1, which is a standard form found in integral tables (R.S. Burington, 1965). Then, after some algebraic manipulation (see Appendix), we obtain the following closed form expression for the angle subtended by the ray in passing through the atmospheric layer at r_i,

$$\psi\,|_{r_i}^{r_{i+1}} = C_0\left[A(F(h_m)-F(0)) + (\sqrt{a+bh_m+ch_m^2}\,B(h_m) - \sqrt{a}B(0))\right] \qquad (10)$$

where for $c < 0$,

$$F(h) = \frac{\sin^{-1}(\alpha(h))}{\sqrt{-c}}, \alpha(h) = \frac{-2ch-b}{\sqrt{b^2-4ab}},$$

and for $c > 0$,

$$F(h) = \frac{1}{\sqrt{c}}\log(2ch + b + 2\sqrt{c}\sqrt{a+bh+ch^2}).$$

Here $B(h)=3h/2cr_i^2 - 2/cr_i - 9b/4c^2r_i^2$ and $A=1 + b/cr_i + 9b^2/8c^2r_i^2 - 3a/2cr_i^2$. The result for the special case $c=0$, along with the modifications necessary for a down-going ray, are given in the Appendix.

The expression (10) is evaluated for each atmospheric layer and the total angle subtended by the ray within the sector, ψ_k, is obtained from

$$\psi_k = \sum_{i=1}^{L^k} \psi\,|_{r_i}^{r_{i+1}} \qquad (11)$$

where L^k is the subset of height layers traversed by the ray within sector k.

In the homing process, the sum of the ψ_k's is calculated for a given ray and is compared to the angle subtended by the sub-satellite point, ψ_s. If the subtended angles differ by less than some preset tolerance level we take that ray as the homed ray and the initial launch angle for the ray, θ_0, is saved. If the difference between subtended angles exceeds the tolerance level a new ray with a different initial angle is launched and the

process continues until the desired ray is found. We discuss the homing procedure in more detail in a later section. In the next section we consider scenarios in which rays may be reflected in atmospheric layers.

3. Ray Turning Points in the Atmosphere (Ducting)

In the previous sections we described the general method for determining rays in the atmosphere. It was implicitly assumed throughout that the rays were launched from the transmitting antenna at initial zenith angles $\theta_0 \leq 90°$ and that the vertical gradients of refractivity were weak in the sense that such initially 'up-going' rays remained up-going , i.e. the local zenith angles $\theta_i \leq 90°$ for all i=1,…, L. In general, however, an initially up(down)-going ray may reverse direction at ray 'turning points' in the atmosphere. In this section we discuss these turning points and describe the method for dealing with them in the ray trace program.

a. Preliminaries

We begin by examining the effect of vertical refractive gradient on ray propagation within the atmosphere. Consider again the scenario shown in Fig.1 and focus on the refractive layer between r_i and r_{i+1}. From equation (3) we can write

$$\begin{aligned} \sin\theta_{i+1} &= \beta_i \sin\theta_i \\ \beta_i &\equiv (\frac{n_i}{n_{i+1}})(\frac{r_i}{r_{i+1}}) \end{aligned} \tag{11}$$

Since $r_{i+1} > r_i$ the layer constant β_i will, in general, be less than or greater than unity depending on the change of the index of refraction in the layer. In the earth's lower atmosphere, the index of refraction is generally a decreasing function of height so we have $n_{i+1} \leq n_i$, where equality holds for a uniform, isotropic atmosphere and by a 'weak' refractive gradient we mean that $n_i/n_{i+1} \approx 1$.

Consider first the scenario discussed earlier which we have termed the 'weak' vertical refractive gradient situation. In this case the constant β_i is less than unity for all layers i=1,..,L and, from equation (11), we see that the local zenith angle at the top of a layer is always less than that at the bottom of the layer. Thus a ray that starts out up-going ($\theta_i \leq 90°$) will remain up-going as it propagates through the atmosphere and we can define a weak vertical refractive gradient as $\beta_i < 1$ or $n_i/n_{i+1} < r_{i+1}/r_i$.

Next consider a ray which is initially down-going as it propagates through the weakly refracting atmosphere. Maintaining our height ordering such that $r_{i+1} > r_i$, we have

$$\begin{aligned} \sin\theta_i &= \beta_{i+1} \sin\theta_{i+1} \\ \beta_{i+1} &= (\frac{n_{i+1}}{n_i})(\frac{r_{i+1}}{r_i}) \end{aligned} \tag{12}$$

where $\theta_{i+1} > 90°$. β_{i+1} is again greater or less than unity depending on the refractive gradient in the layer. In this case, for a weak refractive gradient, $\beta_{i+1} > 1$ for all layers, the local zenith angle on exiting the layer, θ_i, is smaller than the incident angle and we again have $n_{i+1}/n_i > r_i/r_{i+1}$. However, if the local incident zenith angle is very near 90° for some layer, the sine of the exit angle may exceed unity and become undefined. In this case a ray turning point has been reached within the layer and the ray trace is stopped. The local zenith angle, now less than 90°, is determined as described below and the ray trace is re-started from that point. These scenarios for weak refractive gradients, for both up-going and down-going initial rays, are shown in the top panel of Figure 2.

Next consider a scenario in which at least one atmospheric layer has a strong refractive gradient. Then, from equation (11) for an up-going ray, $\beta_i > 1$ for such a layer and the local zenith angle of a ray exiting at the top of the layer is greater than that at the bottom of the layer. Additionally, if the local zenith angle θ_i at the bottom of the layer is less than but close to 90°, the sine of the exiting angle may exceed unity and become undefined. In this instance the ray has turned within the layer and again the ray trace program must deal with the change in the ray trajectory.

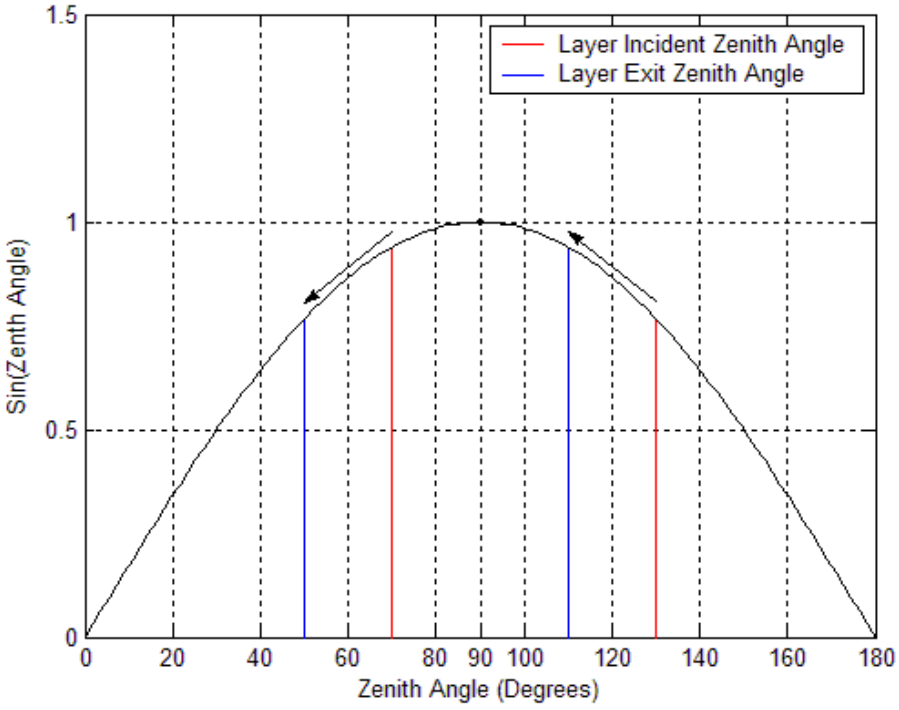

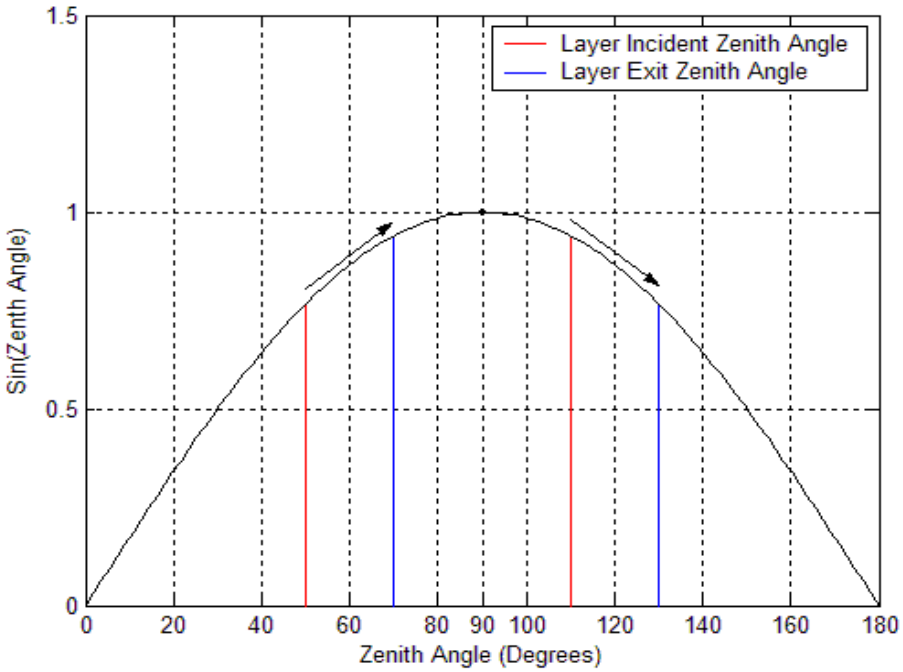

Figure 2. Illustrating the relationship between layer incident and exit angles for (top) a 'weak' refractive layer, and (bottom) for a 'strong' refractive layer. Arrows indicate the direction the zenith angle moves as the ray passes through the layer for each situation.

For an initially down-going ray incident on a layer for which $\beta_{i+1} < 1$, the local zenith angle on exiting the layer will exceed the incident angle. If the layer is near the earth's surface, the ray may hit the earth and the ray trace is stopped. These large refractive gradient scenarios are shown in the bottom panel in Fig. 2 for both up-going and down-going initial rays.

b. Ray methods at turning points

In the previous section we showed that a ray may reverse direction in a refractive layer under some conditions. To determine if such a ray turning occurs in a layer we apply equation (11) for initially up-going rays or equation (12) for down-going rays to each layer. If, for an up-going ray ($\theta_i \leq 90°$) incident on the layer, the local zenith angle at exit (θ_{i+1}) exceeds 90°, the ray has turned at some height r_{90} at which θ=90°, where $r_i < r_{90} < r_{i+1}$. We can determine r_{90} from equation (11) by noting that at the turning height we have

$$1 = (\frac{n_i}{n_{90}})(\frac{r_i}{r_{90}}) \sin\theta_i \,, \qquad (13)$$

where $n_{90}=n_i + s_i(r_{90}-r_i)$. Substituting this expression for n_{90} in equation (13) we find that r_{90} satisfies a quadratic equation which we solve for the turning height. We then restart the ray trace program at that height, adjusting parameters for the now oppositely directed ray. Similar results apply for the initially down-going ray which turns 'up-ward' in the layer. Figure 3 shows a vertical fan of rays launched into a strong refractive duct (shown in the figure). As indicated in Fig. 2, the ray behavior in the duct depends critically on both the incident ray angle and the refractive gradient in the layer.

4. Homing

We indicated earlier that the determination of the ray(s) which connects transmitter and satellite requires a homing procedure. If the satellite lies above the geometric horizon of the transmitter there will, in general, be two rays which connect transmitter to receiver, the direct ray and the earth reflected ray. However, the existence of the reflected ray also requires that the transmitting antenna be elevated above the ground. In this section we describe the homing procedure implemented in this version of the program.

a. Direct ray

By direct ray we mean that ray which propagates directly from transmitter to receiver with no intervening earth or structural interaction. This mode will generally exist if the satellite is above the geometric horizon of the transmitting antenna. It may also exist for a satellite slightly below the horizon if a sufficiently strong refractive gradient exists in a non-uniform atmosphere. This 'beyond-line-of-sight' mode does not exist for a range independent propagation region since a trapped ray remains trapped if there is no horizontal gradient in the refractivity.

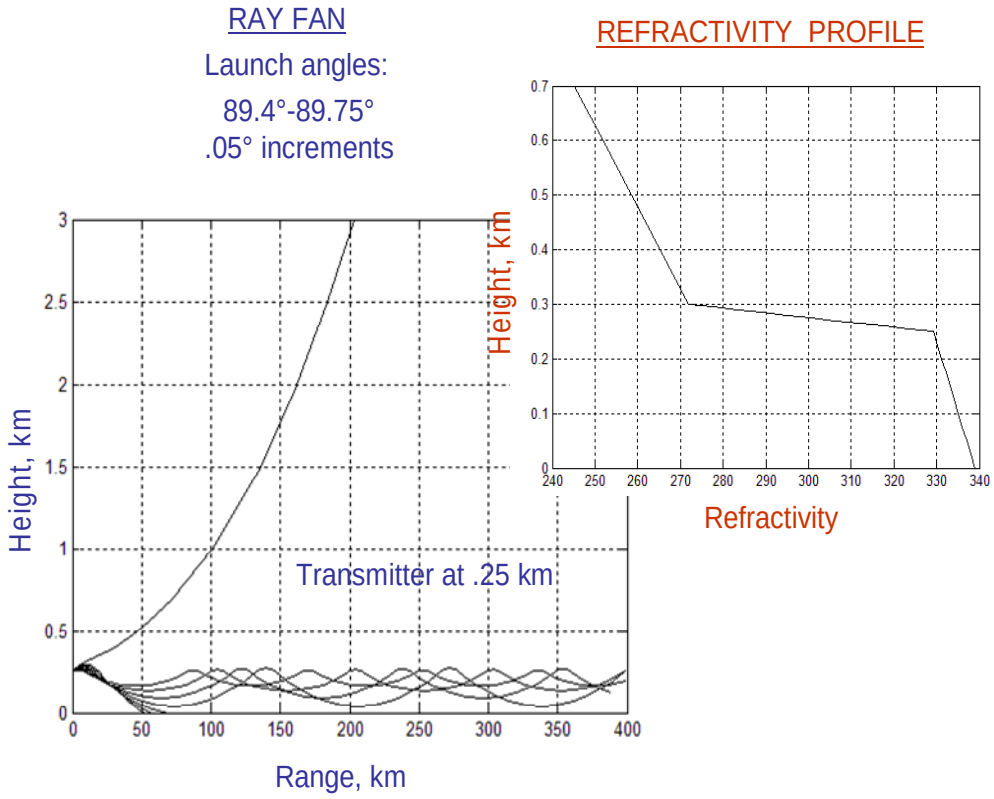

Figure 3. Ray fan launched into a strongly refracting duct. The transmitter lies within the duct and all launch angles are near 90°. Ray behavior in the duct is critically dependent on launch angle and the strength of the duct.

The homing procedure for the direct ray proceeds by a straight-forward iterative procedure involving the launching of rays at prescribed launch angles to the height of the satellite, using the ray equations described above, and comparing the resultant subtended angles (or equivalently, the ground range between the sub-transmitter and sub-ray terminal points) to the angle (ground range) between the transmitter and sub-satellite point. The direct ray is taken to be that ray for which the difference is less than some prescribed tolerance parameter. This procedure has the important advantage of robustness, in that a solution can almost always be found.

The execution time required to locate the direct ray is determined by the number of iterations required to satisfy the specified tolerance which, for the current version is .01 meters in ground range. Clearly, a good initial estimate of the required ray launch angle is crucial in reducing this execution time. Generally speaking, for most transmission angles and refractive conditions, the direct ray differs very little from the straight line path between the transmitter and satellite. For this reason the initial search angle used in the model is the angle corresponding to this straight line path.

The procedure begins by launching a ray at the straight line zenith angle and tracing to the satellite height. If the difference between the required ground range and the spanned ground range is greater than zero the initial launch angle is increased by an initial increment $d\theta$=3° and a new ray is launched. If the initial ground range difference is less than zero the initial launch angle is decreased by $d\theta$ for the next ray. Each time the sign of the range difference changes the launch angle increment is halved and the sign of the launch angle increment is reversed. This procedure continues until the ground range difference falls below the tolerance level.

An illustration of a typical homing procedure for the direct ray is shown in Figure 4. We note the relatively large swings in the difference between the required ground range and the candidate ray ground range. These initially large swings result from the fact that the procedure requires two estimates of range difference to establish the next launch angle. The initial estimate of the straight line launch angle is incremented by a fixed +1° or -1° increment for the second iteration, which provides the estimate for the third iteration. This fixed 1° increment does not necessarily result in a 'good' estimate, as indicated by the scenario shown in Fig. 4.

b. Earth reflected ray

Homing for the reflected ray is significantly more complicated in that it requires a two-dimensional iteration scheme since the location of the reflection point on the earth's surface is not known initially. The requirement for the location of the reflection point is that the reflection angle of the ray, measured relative to the plane tangent to the earth at the reflection point, is equal to the incident angle. This is an approximation to the full theory of the reflection process from a curved surface (reference) which becomes increasingly inaccurate for very low incident angles. We use the approximation here because it provides a fast, acceptably accurate estimate for the homing process in most cases.

The process begins by selection of an initial candidate point for the reflection location on the earth's surface. In most cases, the actual location of the reflection point is close to the transmitter and will generally lie within the refractivity sector nearest to the transmitter site. For the purposes of the homing procedure, the selected candidate reflection point is treated as the transmitter location and direct rays connecting this point to the satellite and actual transmitter location are determined by the method described in the previous section. The launch angles of the determined rays are compared and the candidate location of the reflection point is adjusted based on the difference in the angles. This process continues until a point is determined for which the difference between launch angles for the direct rays to the actual transmitter site and satellite is less than a specified tolerance.

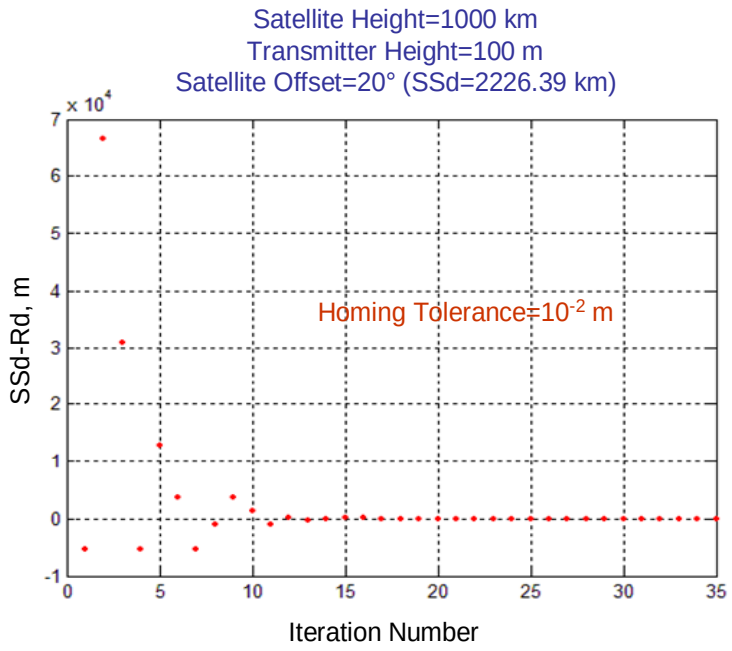

Figure 4. Illustration of the homing process for a typical direct ray determination. Each point represents a candidate ray launched at a different initial angle. The vertical axis is the difference between SSd (= $\psi_s r_e$, ψ_s=20°), the fixed ground distance between the sub-satellite and sub-transmitter points, and the ground range subtended by the candidate ray at each iteration, Rd.

The result of this homing process is the identification of that ray which connects transmitter to satellite. For later processing we also require the total ray length, x, of this ray. The total path length is obtained by summing the individual path length increments, x_i, from each refractive layer. From Fig. 1 we see that the path length increment in the *ith*- layer is given by

$$x_i = \sqrt{r_i^2 + r_{i+1}^2 - 2 r_i r_{i+1} \cos(\psi\,|_{r_i}^{r_{i+1}})}\,. \qquad (14)$$

5. Modifications for Range Dependent Ray Calculations

It has been assumed in all of the above that the refractivity varies in height only. In reality, the earth's refractivity also varies in the horizontal direction (range) and some knowledge of that variation is required for accurate determination of rays, especially for the ducting conditions described earlier. If we consider the instantaneous vertical plane which contains the transmitter location, satellite location and the earth's center, we earlier defined the propagation region as that portion of the plane bounded by radials from the

earth's center through each of the satellite and transmitter locations. Within the propagation region, it is generally true that the earth's refractivity at a fixed height changes as we move within the region. We defined a sector as that portion of the region for which the refractivity is approximately constant as we move in range. Thus a propagation region may be made up of several sectors, within each of which the refractivity varies, approximately, in height only and so all of our previous results are assumed to be valid within a sector. If a ray crosses into different sectors as it progresses to the satellite, we must modify the ray trace to reflect the different refractive environment in each new sector. In this section we describe this process.

Consider the scenario shown in Figure 5, where an up-going ray is shown incident on a layer at height r^k_i, where the superscript denotes the 'k-th' sector and ψ_k is the total angle subtended by the sector. Several scenarios are possible for the ray within the layer. First, if the ray does not reach a turning point in the layer and the total angle subtended in the layer plus the sum of the angles subtended in previous layers does not exceed ψ_k, we continue the ray to the next layer. Second, if a turning point is reached in the current layer we deal with the reflection as described earlier. In this case we sum the angles subtended before and after reflection within the layer and add this to the total angle subtended in the previous layers. Again, if the total does not exceed ψ_k, the ray trace is continued with the ray now going in the opposite direction.

Next we assume that the ray does not reach a turning point in the initial layer but it does pass into the next sector at the transition height r_t (see Fig. 5). To determine the transition height we use an iterative procedure of selecting a candidate height between r^k_i and r^k_{i+1} and calculating the angle subtended by the ray in traversing the 'virtual' layer between r^k_i and the candidate transition height. The subtended angle in the virtual layer is added to the total angle subtended in the lower layers (up-going initial ray) and the result is again compared to ψ_k. Based on the comparison, the candidate transition height is adjusted up or down and the process repeated until the difference between the total angle subtended by the ray up to the transition height and ψ_k is less than some pre-set criteria. Then, applying Bouger's Law, the local zenith angle of the ray at r_t is calculated and the ray is continued at that angle into the next sector. The ray trace then continues as before, using the refractivity profile assigned to the following sector.

The final possibility involves a situation in which the ray not only passes into the next sector within a layer, but also reaches a turning point within the layer. In this case we must calculate the turning point, r_{90}, and transition height, r_t, within the layer to determine which height was reached first. If the turning point is reached before the transition height, the turning occurs before the ray passes into the next sector and the turning of the ray is handled in the usual way within the current layer/sector. The ray, now propagating in the opposite direction is then followed into the next sector as described in the previous paragraph.

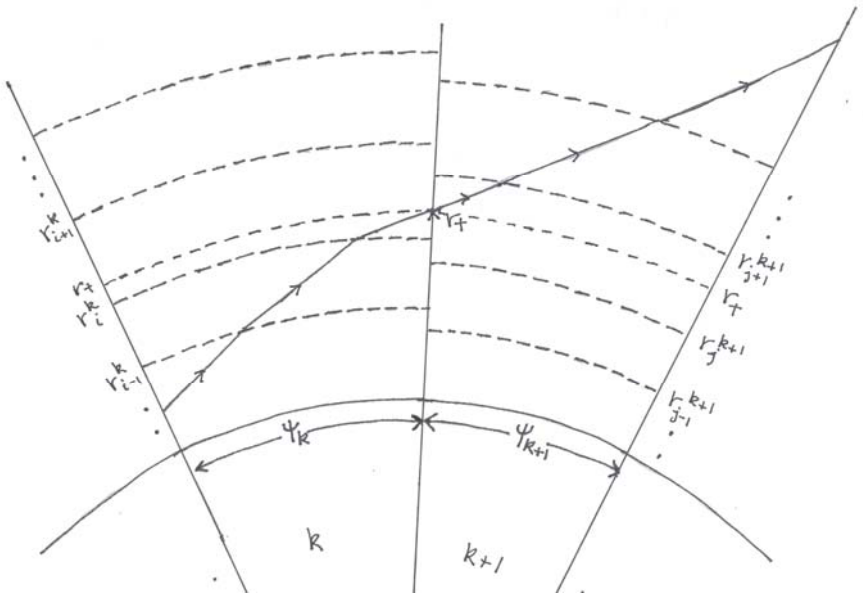

Figure 5. Illustrating ray transition between adjacent propagation sectors. The radial of length r_t (= r_e+h_t) is the transition height between sectors. The angles ψ_k and ψ_{k+1} are the angles subtended by each sector.

If the transition to a new sector occurs at a lower height than the ray turning point, the transition height is determined as described above and the ray continued in the next sector. The ray may or may not reach a turning point in the new sector where a different refractivity profile exists. If it does reflect in the new sector, the usual methods are employed within the new refractive profile for the next sector.

Figure 6 shows a scenario where the propagation region consists of two sectors. The refractivity in the initial sector contains a trapping layer while the second does not. As indicated, the initial fan of rays are all trapped in the duct (top right of Fig. 6). As they propagate to the next sector the rays are no longer bound to the low altitude duct and may escape to reach satellite heights.

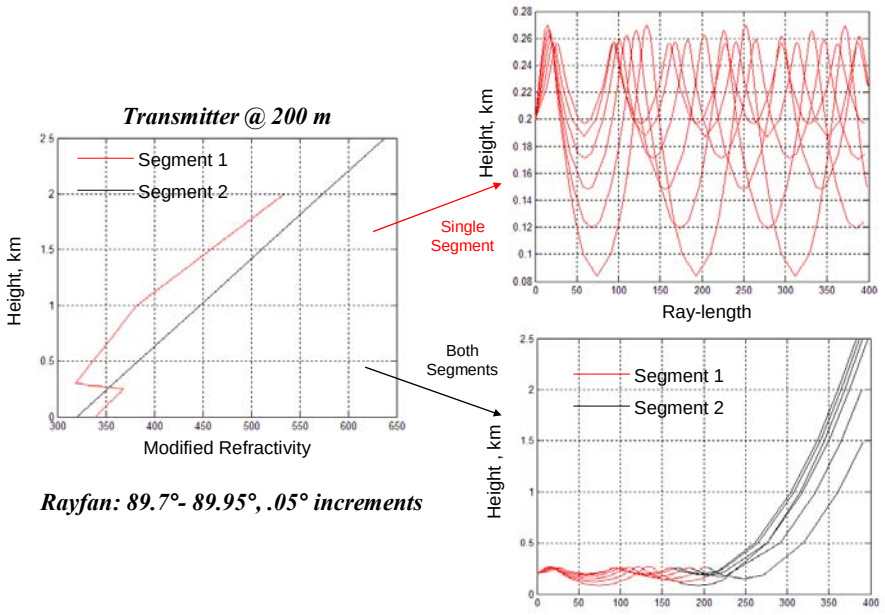

Figure 6. Illustrating the effect on ray propagation of range dependent refractivity. The initial sector contains a ducting profile which traps rays launched within the duct (upper right). When the trapped rays pass into the next non-ducting sector they can escape to satellite heights (lower right).

IV. SATELLITE LOCATION AND TRACKING

Explicit in the previous discussion regarding homing is the assumption that the location (R_s,ψ_s) of the satellite is known whenever one wishes to communicate. While this assumption may be partially true when dealing with geo-stationary satellites, it is certainly not true for low orbiting satellites whose location changes rapidly in time. Such satellites may be available for transmissions from a fixed transmitter site for only a few minutes several times per day and so prior knowledge of those occurrences can be critical for successful system operation.

The accurate prediction of the location of a satellite at any given time requires, first, precise knowledge of its location and orbital velocity at some reference time as near to the required time as possible. This precise information is used as an initial condition for the solution of the orbital equation of motion, which solution provides the time development of the orbit and allows future (and past) satellite locations and velocities to be determined. In time, however, inaccuracies in this process (caused by inaccurate input and/or incomplete knowledge of the forces acting on the satellite) cause the actual satellite location and velocity to deviate from the predicted values. When the difference between actual and predicted satellite location and velocity becomes excessive, a new precise set of input data must be obtained and the process of determining the time dependence of the orbital parameters is repeated.

To determine satellite location for the ESPM^2 we have included two orbital prediction models, designated SGP4 and SDP4, developed for the North American Aerospace Defense Command (NORAD), which is a 'bi-national United States and Canadian organization charged with the missions of aerospace warning and aerospace control for North America. Aerospace warning includes the monitoring of man-made objects in space, and the detection, validation, and warning of attack against North America whether by aircraft, missiles, or space vehicles, through mutual support arrangements with other commands. Aerospace control includes ensuring air sovereignty and air defense of the airspace of Canada and the United States' (http://www.norad.mil). To accomplish this mission, NORAD maintains and publishes the precise satellite location information necessary for the determination of satellite location for all resident space objects (F.R. Hoots and R.L. Roehrich, 1988). This information is available on-line in the form of two-line element sets (TLE) for each satellite. The TLE provides the input data for execution of the orbital prediction models.

The models SGP4, for near earth satellites (orbital period less than 255 minutes) and SDP4 for deep space orbiters, including geo-stationary satellites, require NORAD TLE orbital element files for execution. The driver program selects the appropriate model based on the input data, a process that is transparent to the user. The basic output from the program consists of the satellite location and velocity at the required time in the inertial coordinate system used for the calculations. Documentation of the details of the programs SGP4 and SDP4 are available (F.R. Hoots and R.L. Roehrich, 1988; and references therein) and are not presented here as they are beyond the scope of this document.

For the purposes of the ESPM^2 program, software has been developed for translation of the satellite location to the earth-centered spherical coordinate system which rotates with the earth that is used for ray determination (T.S. Kelso, 1995(a); 1995(b); 1996). Once the location is determined in the proper coordinate system, we can calculate the location (R_s,ψ_s) required for the ray trace homing procedure. We also provide prediction of the times at which the satellite climbs above the local horizon, and is thus available for communication from a given transmitter site for a non-ducting refractive profile. Figure 7 shows example output which combines the satellite tracking software with ESPM^2 to provide estimates of signal strength at the satellite and transmit antenna pointing angles. It should be stressed that a user with independently obtained satellite location data is not required to use the satellite orbit programs described here. However, such location data must be entered in a format consistent with that required by the ESPM^2 software.

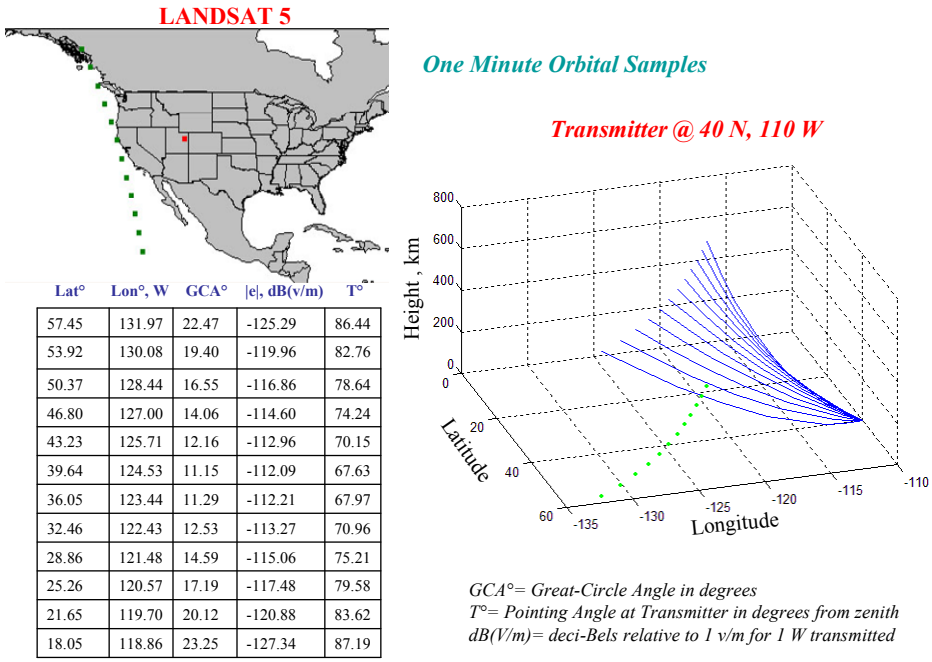

Lat°	Lon°, W	GCA°	|e|, dB(v/m)	T°*
57.45	131.97	22.47	-125.29	86.44
53.92	130.08	19.40	-119.96	82.76
50.37	128.44	16.55	-116.86	78.64
46.80	127.00	14.06	-114.60	74.24
43.23	125.71	12.16	-112.96	70.15
39.64	124.53	11.15	-112.09	67.63
36.05	123.44	11.29	-112.21	67.97
32.46	122.43	12.53	-113.27	70.96
28.86	121.48	14.59	-115.06	75.21
25.26	120.57	17.19	-117.48	79.58
21.65	119.70	20.12	-120.88	83.62
18.05	118.86	23.25	-127.34	87.19

GCA°= Great-Circle Angle in degrees
T°= Pointing Angle at Transmitter in degrees from zenith
dB(V/m)= deci-Bels relative to 1 v/m for 1 W transmitted

Figure 7. Illustration of the use of the satellite orbit determination software with the ESPM[2] ray trace software. Green dots represent the sub-satellite locations for an orbital pass of the LANDSAT 5 satellite. The homed rays are shown in blue. The table contains estimates of signal strength and antenna pointing angles for rays transmitted from the assumed transmitter site.

V. SIGNAL STRENGTH EVALUATION

In the preceding sections we described the ray tracing process and the homing procedure which permits the ray(s) which connect transmitter and receiver to be determined. With this information in hand, we can proceed to the evaluation of the electric field strength at the receiver in order to assess the expected system performance. In this section we derive general equations for the fields and discuss the models used for evaluation of the terms which appear in the equations.

1. General Field Equations

We assume that the total vector field at the satellite position can be written,

$$\vec{E}_t = \vec{E}_d \exp(ik\phi_d) + \vec{E}_r \exp(ik\phi_r), \qquad (15)$$

where $|E_t|$ is the total field, $|E_d|$ is the direct field amplitude, $|E_r|$ is the earth reflected field amplitude, k is the free space wave number and

$$\begin{aligned} \phi_d &= p_d + p_0 \\ \phi_r &= p_r + \arg(R)/k \end{aligned} \tag{16}$$

Here p_0 is the initial phase of the direct ray relative to the reflected ray and $p_{d(r)}$ is the phase path length given by,

$$p_d = \int_t^s n ds_d \, , \; p_r = \int_t^g n ds_r + \int_g^s n ds_r \, , \tag{17}$$

where t is the transmitter location, s is the satellite location and g is the ground reflection point. In this equation, $ds_{d(r),}$ is a ray element along the direct (reflected) ray path, which is determined in the ray trace program, and n is the index of refraction. The method used to determine the phase path is entirely similar to that used for the rays and is outlined in the Appendix. R is the complex Fresnel reflection coefficient which accounts for the effects of a finitely conducting earth, and its formula is provided in the Appendix for both horizontal and vertical polarization.

The reflected field amplitude in (15) is composed of several terms to account for reflections from a non-perfectly conducting, curved-earth surface. Thus we assume the reflected field amplitude can be written,

$$\vec{E}_r = \vec{E}_0 |R| D \, , \tag{18}$$

where $|E_0|$ is the amplitude of a wave reflected from a smooth, flat, perfectly conducting tangent plane at the reflection point after traversing a total distance d_r to the satellite. D is the (real) divergence of the wave due to reflection from a curved earth surface.

From (15) the magnitude of the total field is given by

$$|E_t|^2 = (E_d \exp(ik\phi_d) + E_r \exp(ik\phi_r))(E_d \exp(ik\phi_d) + E_r \exp(ik\phi_r))^* \, ,$$

where the asterisk represents complex conjugate. We set p_0=0 and assume all the fields are co-polarized. Then the field amplitudes can be taken as real scalars and the total field at the satellite is given by

$$E_t^2 = E_d^2 + E_r^2 + 2E_d E_r \cos(k(\phi_d - \phi_r)) \, , \tag{19}$$

where the phase of the reflected wave includes the Fresnel phase as indicated in (16).

Now the power flux density at the satellite in the direct ray, E_d^2/Z_0, is given from the Poynting Theorem by

$$\frac{E_d^2}{Z_0} = p_{tx} g_{tx} l_s l_{ra} l_{ga} \cdots \tag{20}$$

where p_{tx} is the transmitter power (Watts), g_{tx} is the transmit antenna directive power gain relative to isotropic evaluated at the elevation angle of the direct ray at the transmitter, $l_s = 1/4\pi x_d^2$ is the loss due to signal spreading, l_{ra} is loss due to rain attenuation and l_{ga} is loss due to gaseous absorption. Here $Z_0 = 120\pi \sim 377\ \Omega$ is the characteristic impedance of the atmosphere and x_d is the direct ray path length in meters given in equation (14).

For the reflected wave we first write

$$\frac{E_0^2}{Z_0} = p_{tx} g_{tx} l_s l_{ra} l_{ga} \cdots, \tag{21}$$

where E_0 is the field amplitude for a wave reflected from a smooth, flat, perfectly reflecting surface as described above. Here $l_s = 1/4\pi x_r^2$ is the spreading loss for the reflected wave path and the other terms are the same as above with appropriate changes for the different path. The actual reflected wave amplitude is obtained by inserting (21) into (18),

$$\frac{E_r^2}{Z_0} = p_{tx} g_{tx} l_s l_{ra} l_{ga} l_R l_D \cdots , \tag{22}$$

where $l_R = |R|^2 \leq 1$ and $l_D = D^2 \leq 1$.

The total field at the satellite is obtained from equations (16), (17), (19), (21) and (22). In these expressions the loss terms are ratios which are less than unity for a true loss. To obtain l_{ra} from L_{ra}, (the dB value derived in the rain attenuation routine), we use $l_{ra} = 1/10^{**}L_{ra}$. l_{ga} is obtained from L_{ga} in a similar manner.

2. Rain Attenuation Loss

It is well known that absorption due to rain along the propagation path is a major source of signal degradation for earth to satellite communications (book) and we have included a model for estimation of rain loss in the ESPM^2 model. There exists a large body of research on the estimation of the geographical and frequency dependence of rain loss (book) and the International Telecommunication Union (ITU) periodically updates and modifies their recommended model based on this research. For the ESPM^2 module we have chosen to implement the current ITU model (ITU-R P.618-8, P.837-4, P.838-3, P.839-3), which was developed by Dissanayake and Alnutt (A.W. Dissanayake and J.E.

Alnutt, 1992) and has been shown to provide accurate predictions when compared to data collected over long time frames over several frequencies (G.S. Feldhake and L. Ailes-Sengers, 2002).

The ITU model includes a contour map of the maximum height above the earth for which rain is likely to exist (the mean 0° degree isotherm) (ITU-R P.839-3, 2001). This height is evaluated at the transmitter site and only that portion of the ray path lying below the height is included in the loss determination.

The ITU models are statistical in nature and include estimates of rainfall rate exceeded for a given probability of the average year for the transmitter site (ITU-R P-837-4, 2003). For our implementation we have chosen a probability level of .01, leading to a near 'worst case' estimate for long term system planning.

The output of the series of ITU models is an estimate of the attenuation rate for propagation paths in the region of the transmitter. We determine the path loss by multiplying the attenuation rate by the ray path length determined in the ray optics module. The path loss, for both the direct and earth reflected rays, are then used in predicting the final signal strength as described above. A detailed description of the rain attenuation model is outside the scope of this document and the interested reader is directed to the ITU documents for more information.

3. Atmospheric Gaseous Absorption Loss

The frequency dependent loss of signal amplitude due to absorption by molecular species in the atmosphere is another important mechanism that must be included for accurate prediction of signal strength. These losses are produced by resonant interactions of the wave with particular molecular species in the atmosphere.

To calculate the gaseous absorption for a particular ray, we again turn to the ITU recommended model (ITU-R P.676-6, 2005, Annex 1). Unlike the rain attenuation model, the gaseous absorption is a height dependent phenomenon and a gaseous attenuation rate is determined at each layer height equivalent to the height at each level of refractive index input to the ESPM[2]. This data is input to the model along with the refractivity profile and the absorption loss over the entire propagation path is determined for each ray by summing the incremental losses within each layer. The calculation of gaseous attenuation rate is valid from 1 to 1000 GHz. A detailed description of the gaseous absorption model is outside the scope of this document and the interested reader is directed to the ITU documents for more information.

4. Additional Output Parameters: Phase Path Length, Group Path Length and Faraday Rotation

Several parameters of general interest, in addition to the signal strength and antenna pointing angles, can be calculated from the ray trace results. These parameters, which are

obtained by integration along the ray path, include the phase path length, the group path length and the rotation of the plane of polarization (Faraday Rotation).

In general, determination of the signal strength at the satellite requires calculation of the phase path difference between the direct and the earth reflected rays (see equation (19)). Equation (17) defines the phase path length '*p*' for a ray connecting transmitter to satellite as

$$p = \int_t^s n ds \tag{23}$$

where 't' is the transmitter antenna location, 's' is the satellite location and '*ds*' is an element of the homed ray connecting the transmitter and receiver. The total phase path is made up of the sum of contributions from each refractive layer traversed by the ray and so we focus on the contribution of a single layer between $r=r_i$ and $r=r_{i+1}$ and write

$$p_i = \int_{r_i}^{r_{i+1}} n ds_i \tag{24}$$

Following the same procedure outlined earlier, we change the integral along the ray path to one along the radial coordinate *r* (see equation (6)). Then, making similar approximations as in equations (7) and (8), we can write the contribution to the phase path in the layer

$$p_i = n_i^2 r_i \Gamma_1 + 2 n_i r_i^2 \Gamma_2 + s_i^2 r_i^3 \Gamma_3 \tag{25}$$

where Γ_i, i=1,2,3, are defined in equation (9) and the other variables are also defined in the text. Evaluation of Γ_i, i=1,2,3, is outlined in the APPENDIX. The total phase path length is then obtained from the sum of contributions from each layer traversed. These calculations are made for both the direct ray path and the reflected ray path if the mode is calculated.

Another parameter which is generally of interest for trans-ionospheric propagation is the group path delay or group path length, which is simply determined from the group delay by multiplying by the speed of light in vacuum. The group delay represents the time delay for the information modulated onto the carrier wave and is especially important for digital signals transmitted through the ionosphere.

In equations (6) and (8) we defined the approximations used for the atmospheric index-of-refraction in the ray trace application. We note that the index in the atmosphere is not an implicit function of the frequency of the wave. In that case, the group path length and the phase path length are identical. However, an electromagnetic wave that

traverses any part of the earth's ionosphere experiences additional delay and the phase path length and group path length will differ. To derive an expression for group delay

VI. APPENDIX

In the text we claimed that equation (5), the basic ray equation, can be written with equations (7) and (8) as

$$\psi\,|_{r_i}^{r_{i+1}} = C_0\left[\Gamma_1 - \frac{2}{r_i}\Gamma_2 + \frac{3}{r_i^2}\Gamma_3\right]. \tag{A1}$$

The definitions of the Γ_i are given in equation (9) and the form of equation (A1) is obvious from equation (7). In this appendix we wish to outline the derivation of the solution of the ray equation given in equation (10).

We first note that the integrals Γ_2 and Γ_3 can be written in terms of Γ_1 as follows (R.S. Burington, 1965)

$$\begin{aligned}\Gamma_2(h) &= \frac{D(h)}{c} - \frac{b}{2c}\Gamma_1(h),\\ \Gamma_3(h) &= \frac{h}{2c}D(h) - \frac{3b}{4c}\Gamma_2(h) - \frac{a}{2c}\Gamma_1(h)\end{aligned} \tag{A2}$$

where $D(h)=(a+bh+ch^2)^{1/2}$ and a,b,c are defined in the text after equation (9). Inserting Γ_2 and Γ_3 into equation (A1), and with equation (A2), we write (A1) as

$$\psi\,|_{r_i}^{r_{i+1}} = C_0\left[A\Gamma_1(h) + D(h)B(h)\right]_0^{h_m} \tag{A3}$$

where A and $B(h)$ are defined in the text after equation (10). For the case $c < 0$, the integral Γ_1 is given by

$$\Gamma_1(h) = \frac{\sin^{-1}(\alpha(h))}{\sqrt{-c}}, \alpha(h) = \frac{-2ch-b}{\sqrt{b^2-4ab}},$$

and for $c > 0$ we have

$$\Gamma_1(h) = \frac{1}{\sqrt{c}}\log(2ch + b + 2\sqrt{c}\sqrt{a+bh+ch^2}).$$

Note that $\Gamma_1(h)$=F(h) in the text. Evaluation of equation (A3) at the integration boundaries results in equation (10) in the text.

For the special case $c = 0$, the integrals Γ_2 and Γ_3 can again be written in terms of Γ_1, which is given in this case by $\Gamma_1(h)=(2/b)(a+bh)^{1/2}$. Evaluation of equation (A2) leads to

$$\psi\,|_{r_i}^{r_{i+1}} = C_0\left[Q(h)\Gamma_1(h)\right]_0^{h_m}$$

or

$$\psi\,|_{r_i}^{r_{i+1}} = C_0\left[\left(\frac{2}{b}\sqrt{a+bh_m}\right)Q(h_m) - \left(\frac{2}{b}\sqrt{a}\right)Q(0)\right] \qquad \text{(A4)}$$

where $Q(h)=1+2(2a-bh)/3br_i+(8a^2-4abh+3b^2h^2)/5b^2r_i^2$.

Finally, we note that for a down-going ray incident on the refractive layer ($\theta_{i+1} > 90°$) the form of these equations remains the same. However, the signs of the Γ_2 and Γ_3 terms in equation (A1) are reversed. Also, for the coefficients b and c (see text after equation (9)), the sign of the second term in each is reversed. Further we note, in this case, c is always positive.

VII. REFERENCES

K.D. Anderson, 'Determination of Water Level and Tides Using Interferometric Observations of GPS Signals', *J. Atm. Oceanic Tech.*, **17**, pp.1118-1127, Aug. 2000.

R.S. Burington, *Handbook of Mathematical Tables and Formulas, Fourth Ed.*, McGraw Hill, 1965.

G.S. Feldhake, L. Ailes-Sengers, 'Comparison of Multiple Rain Attenuation Models with Three Years of Ka Band Propagation Data Concurrently Taken at Eight Different Locations', *Online J. Space Comm.*, Issue 2, Fall 2002.

F.R. Hoots, R.L. Roehrich, 'Models for Propagation of NORAD Element Sets', *SPACETRACK Report No. 3*, compiled by T.S. Kelso, 31 Dec 1988.

ITU-R Recommendation P.618-8, "Propagation data and prediction methods required for the design of Earth-space telecommunication systems", 2003.

ITU-R Recommendation P.676-6, 'Attenuation by atmospheric gases', 2005.

ITU-R Recommendation P.837-4, 'Characteristics of precipitation for propagation modeling', 2003.

ITU-R Recommendation P.838-3, 'Specific attenuation model for rain use in prediction methods', 2005.

ITU-R Recommendation P.839-3, 'Rain height model for prediction methods', 2001.

J.M. Kelso, *Radio Ray Propagation in the Ionosphere*, McGraw Hill, 1964.

T.S. Kelso, 'Orbital Coordinate Systems, Part I', *Satellite Times*, **2**, no. 1, Sep/Oct 1995(a).

T.S. Kelso, 'Orbital Coordinate Systems, Part II', *Satellite Times*, **2**, no. 2, Nov/Dec 1995(b).

T.S. Kelso, 'Orbital Coordinate Systems, Part III', *Satellite Times*, **2**, no. 3, Jan/Feb 1996.

A.R. Lowry, C. Rocken, S.V. Sokolovskiy, K.D. Anderson, 'Vertical profiling of atmospheric refractivity from ground-based GPS', *Radio Sci.*, **37**, (3), pp. **13**-1-**13**-10, 2002.

REPORT DOCUMENTATION PAGE

Form Approved
OMB No. 0704-01-0188

PLEASE DO NOT RETURN YOUR FORM TO THE ABOVE ADDRESS.

1. REPORT DATE *(DD-MM-YYYY)*	2. REPORT TYPE	3. DATES COVERED *(From - To)*
May 2008	Final	

4. TITLE AND SUBTITLE

Ray-Optics-Based Signal Strength Prediction Method for the Earth-to-Satellite Propagation Model with Meteorology (ESPM2) in the Advanced Refractive Effects Prediction System

5a. CONTRACT NUMBER

5b. GRANT NUMBER

5c. PROGRAM ELEMENT NUMBER

6. AUTHORS

R. Sprague

5d. PROJECT NUMBER

5e. TASK NUMBER

5f. WORK UNIT NUMBER

7. PERFORMING ORGANIZATION NAME(S) AND ADDRESS(ES)

SSC Pacific
San Diego, CA 92152–5001

8. PERFORMING ORGANIZATION REPORT NUMBER

TD 3227

9. SPONSORING/MONITORING AGENCY NAME(S) AND ADDRESS(ES)

Office of Naval Research (Code 322)
800 North Quincy Street
Arlington, VA 22217-5660

10. SPONSOR/MONITOR'S ACRONYM(S)

ONR

11. SPONSOR/MONITOR'S REPORT NUMBER(S)

12. DISTRIBUTION/AVAILABILITY STATEMENT

Approved for public release; distribution is unlimited.

13. SUPPLEMENTARY NOTES

14. ABSTRACT

The Advanced Refractive Effects Prediction System (AREPS) was initially developed as a performance assessment and system analysis tool for the U.S. Navy radar systems operating in the 100- to 20-GHz frequency range. Recently, under majority funding from ONR, AREPS capabilities have been extended to include high frequency (HF), 2- to 30- MHz point-to-point and coverage predictions that support military communications systems and a three-dimensional ionosphereic ray tracing capability for research-oriented and HF system design applications. SPAWAR Systems Center San Diego (SSC San Diego) recently developed a medium-frequency (MF), 300-kHz to 2MHz prediction capability for coverage analysis in the amplitude modulation (AM) radio band. With these additions, SSC San Diego, has extended the AREPS usable prediction frequency range from 300 kHz to 57 GHz and has added significant communications system analysis capability. This report describes the latest efforts to extend the range of AREPS applications to earth-satellite communications. The new capability will be called Earth-to-Satellite Propagation Model with Meteorology (ESPM2) and will employ a ray of optics propagation tool, including available meteorological/refractivity data, to predict signal strength at satellite locations.

15. SUBJECT TERMS

Mission Area: Communications Technology

Atmospheric refractivity, direct ray, ground terrain profile, range-independent refractivity, signal strength evaluation, earth reflected ray, ray turning points, homing.

16. SECURITY CLASSIFICATION OF:			17. LIMITATION OF ABSTRACT	18. NUMBER OF PAGES	19a. NAME OF RESPONSIBLE PERSON
a. REPORT	b. ABSTRACT	c. THIS PAGE			Amalia Barrios
U	U	U	UU	31	19B. TELEPHONE NUMBER *(Include area code)* 619-553-1429

Approved for public release; distribution unlimited.

SSC Pacific
San Diego, CA 92152-5001